DOI: 10.48011/sbse.v1i1.2161

# Electric Potential Calculation in Substation Fences

**Rooney R. A. Coelho*** **Mauricio B. C. Salles†*** **Luciano Martins Neto‡** **José Roberto Cardoso***

* *Laboratory of Applied Electromagnetics* (LMAG)
*Polytechnic School of the University of São Paulo, São Paulo, Brazil*
† *Laboratory of Advanced Electric Grids* (LGrid)
*Polytechnic School of the University of São Paulo, São Paulo, Brazil*
‡ *Federal University of Uberlândia, Minas Gerais, Brazil*

e-mails: *rooneycoelho@usp.br, mausalles@usp.br, lmn@ufu.br, jose.cardoso@usp.br*

**Abstract:** As referred to the safety of people, the metallic fence of a substation is an object of special care. The substation fence is subject to a potential rise as well as to direct contact with people and animals, which is a hazardous situation. The connection of the fence to the substations grounding grid, the sectioning of the fence through isolated parts and the design of a specific fence grounding system are then necessary items for a well-designed project. This paper presents the procedure for calculating the potential rise in a metallic fence, also a report of good fence designing practices, verifying such procedure with an example from the literature.

*Keywords:* Grounding; uniform soil; fences; substations; numerical methods.

## 1. INTRODUCTION

Metallic fences surrounding electrical installations or under areas which may be energized (e.g., a transmission line cable falling over the fence) are grounded aiming to protect people who may come into contact and experience an electric shock. The grounding of fences and gates also intends to protect people from the transferring of hazardous potentials between the substation mesh and remote points, which would result in exposing people to a hazard situation.

Since the touch voltage is due to an electric potential gradient, it is attempted to reduce the potential difference between the soil in the fence vicinity and the potential in the fence itself. This is done in the grounding system project. As shown in Figure 1, when connected to the grounding mesh, the fence is under the same potential as such mesh. In contrast, for the case where the fence is not connected to the mesh, fence posts (or posts and a combination of cables and rods) serve as a grounding system. In such a case, the electric potential of the fence is unknown and needs to be somehow calculated.

The same reasoning can be made for a fence that is separated into sections, where part of the fence can be electrically connected to the mesh and another one isolated from it. When something is connected to the mesh it is referred to as an active electrode, when it is not, as a passive electrode.

Buried metallic objects are under the same electric potential, regardless of current injection. Thus, if there is such object in the vicinity of a grounding system, where a short circuit current flows through the ground, its potential

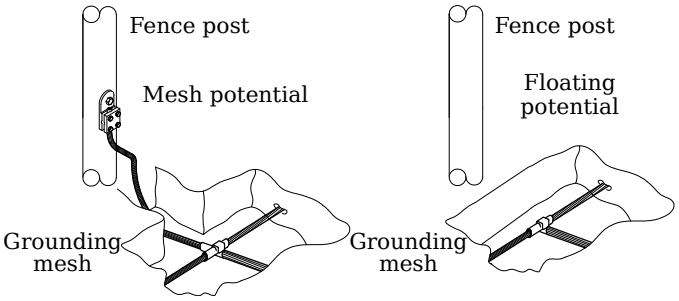


Figure 1. Situations for electric potential rise in a substation metallic fence.

depends on the current intensity, geometry and the distance from the grounding system. Furthermore, it can be stated that the potential has been "transferred" from the grounding system for such object through the ground. This problem can also be interpreted as a conductive coupling between the grounding system and the metallic object.

For Gazzana et al. (2019) numerical and analytical methods are both employed in the determination of surface potentials generated by a grounding mesh. The use of numerical methods for such calculation is, however, more accurate because they circumvent analytical methods limitations (e.g., simple geometries and uniform soils).

This paper presents a calculation procedure for current distribution along electrodes and the electric potential rise in grounding systems involving nearby metallic fences. The aim of this paper is to determine the touch voltage along the fence perimeter, as well as to present mitigating strategies for such dangerous voltages.

## 2. THE MODEL EQUATION SET

In order to define the potential rise in passive electrodes, it is required the development of a model for the grounding system, also the calculation of the electric potential and electrode current distribution.

### *2.1 The electric potential of a linear electrode*

The electric potential, assuming zero at infinity, generated by a point current source $I$, immersed in a uniform resistivity soil $\rho$ is given by

$$V(\boldsymbol{r}) = \frac{\rho I}{4\pi}\left(\frac{1}{\mathcal{R}} + \frac{1}{\mathcal{R}'}\right), \tag{1}$$

with $r_{xy} = \sqrt{(x-x')^2 + (y-y')^2}$, being $\boldsymbol{r}$ the vector position for the calculation point. The distances from both real and image sources to the calculation point are respectively

$$\mathcal{R} = \sqrt{r_{xy}^2 + (z-z')^2} \quad \text{e} \quad \mathcal{R}' = \sqrt{r_{xy}^2 + (z+z')^2}.$$

Including a line segment of length $L$ with uniform current density per unit length rather than a point source, it is possible to integrate the potential generated by the point source along a path between the $\langle x_1, y_1, z_1\rangle$ and $\langle x_2, y_2, z_2\rangle$ coordinates, which respectively represent the line start and endpoint. Using vector notation, this same element can be described as delimited by $\boldsymbol{r}_1$ and $\boldsymbol{r}_2$.

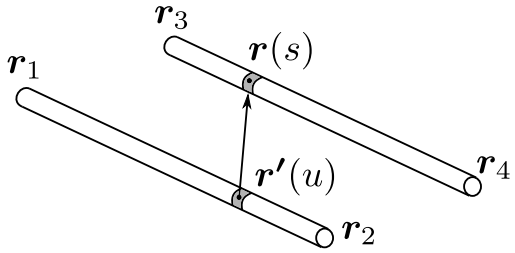


Figure 2. Calculation of the potential generated by the electrode. The current crossed electrode is along $\boldsymbol{r}_1$ and $\boldsymbol{r}_2$. The potential is calculated on another conductor surface, which is located between $\boldsymbol{r}_3$ and $\boldsymbol{r}_4$.

Every point in the line segment is parameterized by variable $u$, such that $u\boldsymbol{r}_1 + (1-u)\boldsymbol{r}_2$ being $u \in [0,1]$ (cf. Figure 2). After calculating the line integral for parameter $u$, the resulting potential is then obtained by (2) (Coelho, 2019).

$$V(\boldsymbol{r}) = \frac{\rho I}{4\pi L}\left(\ln\left|\frac{2a + b + 2\sqrt{a(a+b+c)}}{b + 2\sqrt{ac}}\right| + \ln\left|\frac{2a' + b' + 2\sqrt{a'(a'+b'+c')}}{b' + 2\sqrt{a'c'}}\right|\right), \tag{2}$$

being the auxiliary functions for the real source

$$\begin{aligned} a = a' &= (x_2-x_1)^2 + (y_2-y_1)^2 + (z_2-z_1)^2 = L^2 \\ b(x,y,z) &= 2(z_1-z)(z_2-z_1) + 2(y_1-y)(y_2-y_1) \\ &\quad + 2(x_1-x)(x_2-x_1) \\ c(x,y,z) &= (x-x_1)^2 + (y-y_1)^2 + (z-z_1)^2, \end{aligned}$$

and for the image source

$$\begin{aligned} b'(x,y,z) &= 2(-z_1-z)(z_1-z_2) + 2(y_1-y)(y_2-y_1) \\ &\quad + 2(x_1-x)(x_2-x_1) \\ c'(x,y,z) &= (x-x_1)^2 + (y-y_1)^2 + (z+z_1)^2. \end{aligned}$$

Noteworthy is since (2) is parameterized as a function of segment coordinates, it represents a generic equation for any linear electrode configuration. There is a parameter in (2) that must be imposed, which is the electrode electric current. For multiple electrodes system, the current is non uniformly distributed between electrodes and is determined in such a way that achieves an equipotential surface for the entire conductor association.

## 3. COUPLING BETWEEN ELECTRODES

Since the electrodes are formed by a conductive surface, it is known that such surface is equipotential; the conductors are also interconnected, therefore, under the same electric potential. By applying the superposition theorem, it is possible to determine the current in each electrode in such a way that achieves an equipotential condition. Once the current at each electrode is known, the electric potential, at any point in space, is calculated by superimposing (2) for each electrode in the system.

The potential rise generated by an $i$ segment on the surface of a $j$ segment, for a still to be determined current in $i$, can be calculated by integration, as shown in Figure 2. Once $j$ segment is delimited between $\boldsymbol{r}_3$ and $\boldsymbol{r}_4$, any point in such element can be parameterized as $s\boldsymbol{r}_3 + (1-s)\boldsymbol{r}_4$ for $s \in [0,1]$. The ratio between the potential rise in segment $j$ and the current that generated such potential (from segment $i$) is known as the mutual resistance between segments and is given by the following numerical integration

$$R_{ij} = \frac{\rho}{4\pi L}\int_0^1 \left(\ln\left|\frac{2a + b(s) + 2\sqrt{a(a+b(s)+c(s))}}{b(s) + 2\sqrt{ac(s)}}\right| + \ln\left|\frac{2a' + b'(s) + 2\sqrt{a'(a'+b'(s)+c'(s))}}{b'(s) + 2\sqrt{a'c'(s)}}\right|\right) ds. \tag{3}$$

The case in which $i = j$, represents the resistance of the segment itself. Since the calculation point is taken on its surface, the radius $r_c$ is added for such element by applying a correction in (4), thus shifting the calculation point to the conductor surface.

$$\begin{aligned} x_3 &= x_1 + r_c\frac{y_2-y_1}{L} & x_4 &= x_2 + r_c\frac{y_2-y_1}{L} \\ y_3 &= y_1 + r_c\frac{z_2-z_1}{L} & y_4 &= y_2 + r_c\frac{z_2-z_1}{L} \\ z_3 &= z_1 + r_c\frac{x_2-x_1}{L} & z_4 &= z_2 + r_c\frac{x_2-x_1}{L} \end{aligned} \tag{4}$$

The mutual resistance between segments is used to determine the current distribution for the electrodes.

### *3.1 Active electrode model*

The potential rise $V_0$ calculated on a $i$ segment is the superposition of effects from all $N$ electrodes on such element. The concept of mutual resistance between conductors is used for achieving (5), which is an expression for the electric potential $V_0$ on an active segment.

$$\sum_{j=1}^{N} R_{ij} I_j = V_0 \qquad \text{ou} \qquad \sum_{j=1}^{N} R_{ij} I_j - V_0 = 0 \tag{5}$$

The active electrode model is rooted on the continuity equation (6) as described in Cardoso (2010). For such kind of element, it is imposed the sum of every current from the association equal to the injected current, i.e., the fault current.

$$\oint \boldsymbol{J} \cdot \mathrm{d}\boldsymbol{S} = \sum_{k=1}^{N_p} I_k = I_{\mathrm{cc}} \tag{6}$$

The system ground resistance is achieved by the ratio between the potential rise $V_0$ on electrodes and the total current $I_{\mathrm{cc}}$ injected into the electrodes system.

### *3.2 Passive Electrode Model*

The floating potential $V_p$ on a passive electrode $k$ is calculated by the superposition of effects of all electrodes on such element, both the active($N_a$) and passive ($N_p$) ones.

$$\sum_{j=1}^{N_a+N_p} R_{kj} I_j = V_p \quad \text{ou} \quad \sum_{j=1}^{N_a+N_p} R_{kj} I_j - V_p = 0 \tag{7}$$

This approach can be generalized for several passive electrodes, each electrically isolated from each other. Therefore, it is achieved a similar expression for electrodes of this type.

For the passive electrode model, uniquely from active electrodes, the currents flowing through the electrode through soil may assume negative values, however, the sum of currents is always zero. For a better representation of the current distribution at those elements, it is necessary to perform segmentation on such electrodes.

$$\oint \boldsymbol{J} \cdot \mathrm{d}\boldsymbol{S} = \sum_{k=1}^{N_p} I_k = 0 \tag{8}$$

The mutual resistance between the grounding system and a passive electrode is obtained by the ratio between the potential rise $V_p$ on such electrode and the total current $I_{\mathrm{cc}}$ that has been injected into the grounding system.

### *3.3 Determining the electrode current distribution*

Since the linear electrode equation is described, both active, where there is a current injection, and passive, whose potential is floating, it is possible to determine the system current distribution. Therefore, this article subtly improves the models of Pereira F$^{\mathrm{o}}$ (1999) and Aleixo (2002), adding several passive elements into the formulation, each of them electrically isolated from the others.

It is assumed $n$ as the total number of elements, both active and passive, and $m$ being the number of passive electrodes. The subsequent steps are performed in order to determine the system coefficient matrix:

(1) The mutual resistance between active, passive and between both electrodes is calculated. A $n$ *timesn* block is then formed from those couplings.
(2) For the $n+1$ column, adjacent to the mutual resistance block, each element is -1 if the element index refers to an active electrode or 0 for a passive electrode. Elements not aligned with the mutual resistance block at this column are also null.
(3) If the element index refers to an active electrode, every line term from $n+2$ to $n+m+1$ is null.
(4) For the $n+k+1$ line, where $k$ refers to a passive electrode, it is assumed -1 for each line column that refers to this particular electrode. Thus, those elements are assumed as electrically connected, therefore, under the same floating potential.
(5) When the element index refers to a passive electrode, all the terms from $n+1$ to $n+m+1$, except for the term $n+k+1$, are null.
(6) The lines from $n+1$ to $n+m+1$ are assigned 1 if the column refers to the analyzed grouping index, otherwise it is assigned 0. The line $n+1$ refers to active electrodes, the $n+2$ to the first passive electrodes group, and so on up to $n+m+1$, which refers to the last passive electrode grouping line.
(7) Since the columns from $n+1$ to $n+m+1$ of rows between $n+1$ to $n+m+1$ do not refer to element indexes, all those values are null.

For active electrodes, $V_0$ is assumed for the electric potential. On the other hand, $V_{pk}$ is assumed for the passive electrodes potential, being $k$ and index for such electrodes, ranging from 1 to m. Equation (9) presents the linear system to be solved.

$$\boldsymbol{A} \cdot \mathbf{x} = \mathbf{b} \ , \tag{9}$$

The coefficient matrix $\boldsymbol{A}$ is assembled using the previously described procedure.

$$\mathbf{A} = \begin{bmatrix}
R_{11} & R_{12} & R_{13} & & R_{1k} & & R_{1n} & -1 & 0 & \cdots & 0 \\
R_{21} & R_{22} & R_{23} & \cdots & R_{2k} & \cdots & R_{2n} & -1 & 0 & \cdots & 0 \\
R_{31} & R_{32} & R_{33} & & R_{3k} & & R_{3n} & -1 & 0 & \cdots & 0 \\
 & \vdots & & & \vdots & & \vdots & \vdots & \vdots & & \vdots \\
R_{k1} & R_{k2} & R_{k3} & \cdots & R_{kk} & \cdots & R_{kn} & 0 & -1 & \cdots & 0 \\
 & \vdots & & & \vdots & & \vdots & \vdots & \vdots & & \vdots \\
R_{n1} & R_{n2} & R_{n3} & \cdots & R_{nk} & \cdots & R_{nn} & 0 & 0 & \cdots & -1 \\
1 & 1 & 1 & \cdots & 0 & \cdots & 0 & 0 & 0 & \cdots & 0 \\
0 & 0 & 0 & \cdots & 1 & \cdots & 0 & 0 & 0 & \cdots & 0 \\
 & \vdots & & & \vdots & & \vdots & \vdots & \vdots & & \vdots \\
0 & 0 & 0 & \cdots & 0 & \cdots & 1 & 0 & 0 & \cdots & 0
\end{bmatrix}$$

The vector of unknowns $\mathbf{x}$ is given by

$$\mathbf{x} = \begin{bmatrix} I_1 & I_2 & I_3 & \cdots I_k & \cdots I_n & V_0 & V_{p1} & \cdots & V_{pm} \end{bmatrix}^T,$$

and the system solutions vector $\mathbf{b}$ is given by

$$\mathbf{b} = \begin{bmatrix} 0 & 0 & 0 & \cdots & 0 & \cdots & 0 & I_{\mathrm{cc}} & 0 & \cdots & 0 \end{bmatrix}^T.$$

At the assembling of $\mathbf{b}$ only the term $n+1$ is non-null and is equal to the total system current. With the solution of (9) all electrodes current and potential rise, both active and passive, are simultaneously obtained.

Each passive electrode is formed by an association of segments under the same floating potential, i.e., there are $m$ floating potentials and an electrode grouping for each of them. If the passive electrode is segmented, a current is calculated for each segment, thus increasing the system order. The lines of the system can be exchanged; however,

it was proceeded the aforementioned way, systematizing the interpretation of both active and passive electrodes.

## 4. MITIGATION OF HAZARDOUS VOLTAGES

Substation fences or areas subjected to an eventual energization should be grounded to protect both worker and electrical installation. According to IEEE Std 80 (2015), there are four ways to design the grounding system of a substation fence:

(1) Fence within the substation mesh area and electrically connected to the grounding mesh.
(2) Fence outside mesh area but electrically connected to this mesh.
(3) Fence outside the substation mesh area and not connected to it. The fence is connected to a separate grounding system.
(4) Fence outside the substation area, not connected to the mesh and without a separate grounding system. The electric contact of the fence with the soil occurs only through the fence posts.

According to the Brazilian standard NBR 15751 (2013), metallic fences located inside the substation area must be connected to it at regular intervals, achieving an equipotential condition. Metal fences located outside the mesh-covered plane should be sectioned off from the rest of it, each section being connected at several points and to distinct mesh squares. Each insulated section of the fence must be grounded trough two rods.

The aim of such sectioning is to avoid the transfer of hazardous potentials to distant points and to make fence potential follow the soil potential profile. If any part of the fence crosses the mesh area, this section should be isolated from the rest. Fences beneath transmission or distribution lines must be sectioned too, aiming not to transmit dangerous potentials through its extension if the feeder falls over the fence.

The fence electric contact to soil only by posts, without a dedicated grounding system, will lead to high potential gradients in the proximity of the fence, thereby increasing step and touch voltages, especially when the fence is connected to the mesh. A grounding system for the fence consisting mainly of buried cables is most appropriate in this situation as it softens the nearby soil potential profile.

There is a decreasing of grounding resistance due to the rise of systems effective area when the fence is electrically connected to the mesh. However, there is hazardous potential transfer to the fence and its touch voltage must be kept under control. A peripheral conductor can be buried neighbouring the fence to reduce potential gradients due to such connection with the mesh.

## 5. RESULTS

This paper analyses the grounding system of a 150/20 kV substation, as shown in Figure 3. This example was based on Datsios et al. (2014). The provided short circuit current was 24.75 kA and the soil was assumed as uniform with 87.1 $\Omega.m$ resistivity. The mesh consists of 120 m $^2$ diameter copper conductors and 17 mm diameter with 3 m long copper rods, both buried at 0.6 m depth.

The studied substation has a metallic fence surrounding its outer perimeter with approximately 390 m in length, its distance from mesh ranges between 1.2 m and 23.7 m. This fence is grounded through an individual grounding system, which consists of a horizontal conductor buried at 0.6 m depth.

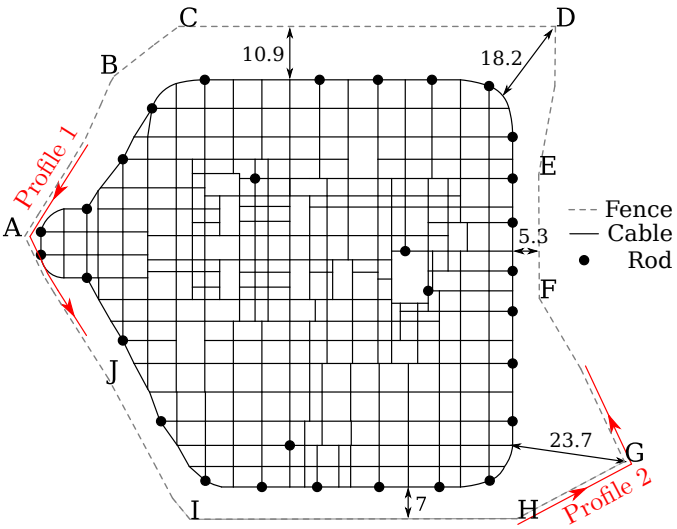


Figure 3. Configuration of the studied grounding system.

Figure 3 also presents two profiles indicating the measurement lines employed by Datsios et al. (2014). Such lines are used as a comparison basis between the method presented herein and the software used by the original article. The letters in figure identify locations referenced on later simulations.

### *5.1 Results Comparison*

In this section, the results of Datsios et al. (2014), which uses the commercial software XGSLab, specifically the Grounding System Analysis (GSA) package, are compared to results achieved using the methodology of this paper.

Table 1. Comparative board.

| | Proposed | Datsios et al. (2014) | Deviation |
|---|---|---|---|
| $R_t$ | 0.443 Ω | 0.458 Ω | 3.34% |
| $V_{\text{mesh}}$ | 10.96 kV | 11.34 kV | 3.38% |
| $V_{\text{fence}}$ | 6.99 kV | 7.32 kV | 4.52% |
| $R_t^*$ | 0.389 Ω | 0.378 Ω | 2.86% |

Table 1 shows the comparison between the results obtained with the presented approach and the values of Datsios et al. (2014). The value of $R_t$ means the grounding resistance when the fence isolated from the mesh, $R_t^*$ the grounding resistance when the fence is electrified, $V_{\text{mesh}}$ and $V_{\text{fence}}$ are the potential rises in the mesh and fence respectively when both are electrically isolated. The deviations between the results of this paper when compared to the original article are low, even with both papers employing different calculation approaches.

Figure 4 shows the touch voltage for the measurement line specified by Profile 1 of Figure 3, while Figure 5 the touch voltage for Profile 2 of the same figure.

The first profile represents a measurement line inside the substation and the second an outside line. Both measurements are performed 1.2 m far from the substation fence,

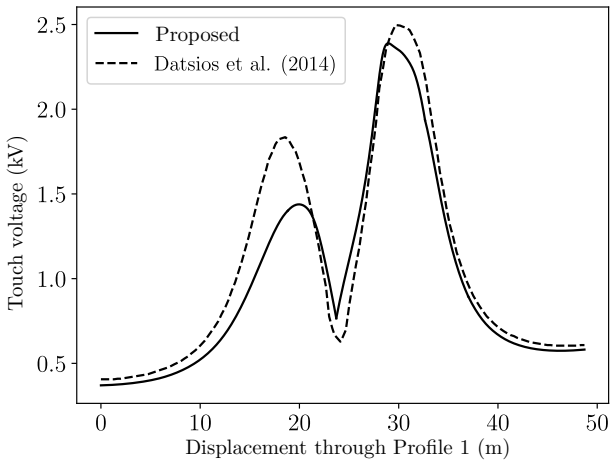


Figure 4. Analysis of Profile 1 of Figure 3.

besides the standard distance imposed by IEEE Std 80 (2015) is one meter for touch and step voltages.

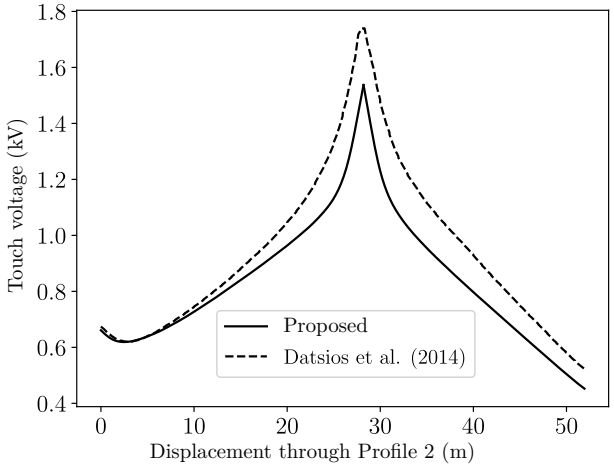


Figure 5. Analysis of Profile 2 of Figure 3.

The touch voltage was calculated in relation to the fence when not connected to the grounding grid, considering the fence without insulated sections. The results obtained are reasonable when compared to those of Datsios et al. (2014).

### *5.2 Touch voltage along the fence*

This section aims to examine the touch voltage for possible electric chock situations. It is studied the influence of the mesh and fence connection. It is also used the standard distance of one meter to express a person's arm length.

As a comparison basis, Figure 6 correlates the touch voltage over the entire fence length to one meter far internal measurement line. Figure 7 also compares the touch voltage along with fence length but from an outside measurement line one meter far instead. Both figures show a comparison between the fence touch voltage, when connected to the mesh and for the case where there is no connection, i.e., a floating potential for fence grounding system.

Since the fence is hugely far from the mesh in major part of the substation, its mesh connection generates a very high

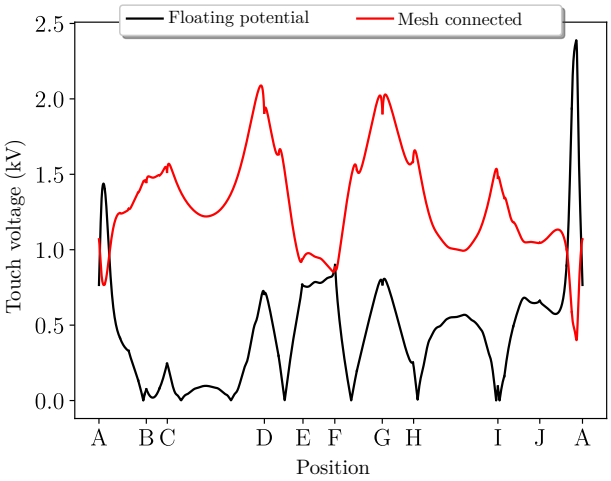


Figure 6. Inside perimeter at 1 m from the fence.

touch voltage, except for the region in the proximity of point A, where the fence is very close.

As expected, the touch voltage that a person is subjected to is higher when taken from outside the substation. Since the touch voltage limit calculated by Datsios et al. (2014) is 1.15 kV (10 cm gravel for coating), it implies a troubling situation, especially for the outside region when the fence is connected to the mesh.

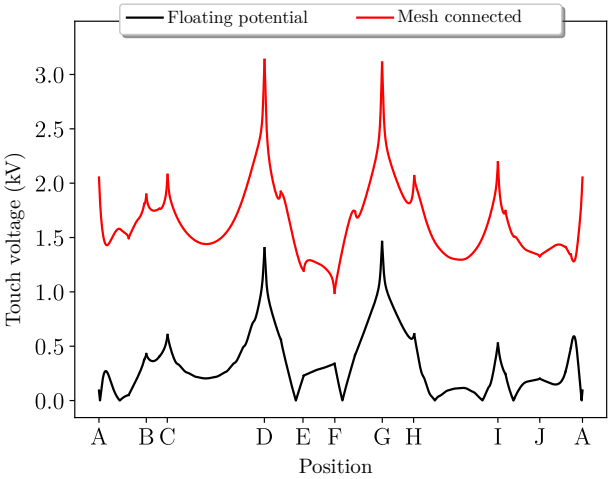


Figure 7. Outside perimeter at 1 m from the fence.

### *5.3 Fence sectioning effect Investigation*

The paper of Datsios et al. (2014) proposes the sectioning of the studied substation fence at the ends of Profile 1 of Figure 3, because a transmission line crosses such region. For the sake of comparison, this work simulates multiple fence sectioning, one for each marker in Figure 3.

Figure 8 presents results for simulated configurations, regarding an outside measurement line and for distinct fence sectioning. Each segment was considered as a floating potential. It is possible to observe the touch voltage discontinuity effect near segmentation points. Note that multiple segmentation reduced such touch voltage for the farthest regions, such as segments $\overline{BC}$, $\overline{CD}$ and $\overline{FG}$, $\overline{GH}$, $\overline{HI}$. Closer regions like $\overline{AB}$ and $\overline{JA}$ have the greatest reduction in touch voltage when considering the fence as unsegmented.

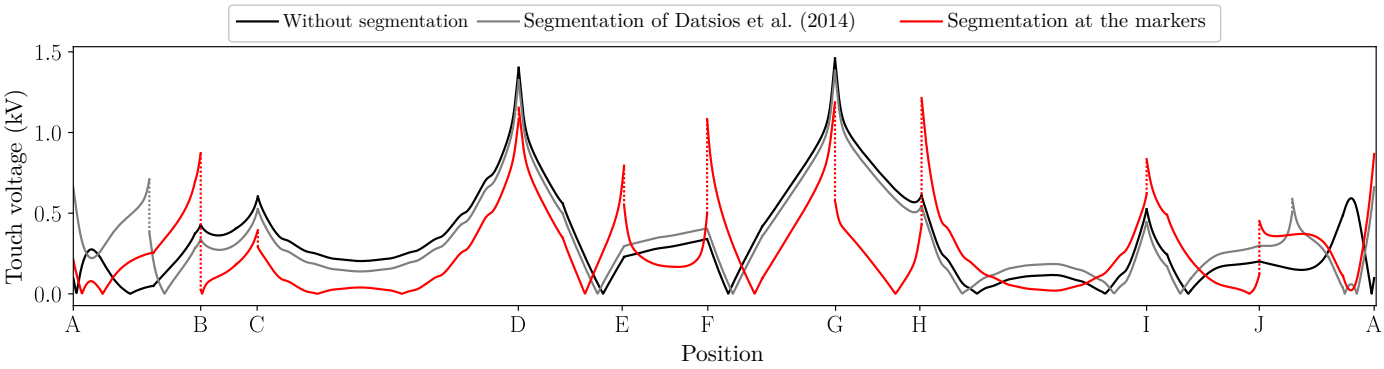

Figure 8. Outside perimeter at one meter from the fence and different segmentation points.

The sectioning of the fence should be done to isolate its farthest regions, imposing the fence potential to follow the soil potential profile, aiming to reduce potential gradients. When the fence is closer to the mesh it is better to keep it continuous. When taking into account only the inside measurement line, as illustrated in Figure 6, connecting the fence to the mesh greatly reduces the touch voltage at its near regions. The safety level relative to the outside of the fence can also be increased by changing the surface covering material, such as building a sidewalk or even to asphalt soil surrounding the substation fence. The fence can also be built in masonry for hazardous regions, mitigating the electric shock by preventing from electrical contact.

## 6. CONCLUSION

This paper presented a calculation procedure for induced potentials in substation fences, as well as strategies for mitigating hazardous voltages. The paper confronted the results of Datsios et al. (2014), which uses proprietary software and is rooted in another calculation method (Partial Element Equivalent Circuit Model); however, both results are similar. The referred paper does not aim at simulation performance, but our proposed procedure is computationally efficient and with considerably simple computational implementation.

The paper generalized the method for distinct configurations, allowing to simulate multiple fence sections either isolated or electrically connected to the grounding mesh. The procedure addressed in this article was applied in a case study extracted from the literature, expanding the original study to include the effect of multiple fence segmentation.

The computational tool presented in this article has great value for substation designers, allowing them to carry out projects considering, e.g., a later substation expansion. In addition, it is also possible to determine an appropriate location for a fence segmentation as well as suitable sections to be connected to the mesh and hazardous locations which may require project readjustment.

## REFERENCES


Aleixo, A.N. (2002). *Análise simultânea de sistemas de aterramento e distribuição de corrente de curto-circuito.* Master's thesis, Escola Politécnica, Universidade de São Paulo- USP.

Cardoso, J.R. (2010). *Engenharia eletromagnética.* Elsevier, Rio de Janeiro, 1 edition.

Coelho, R.R.A. (2019). *Uma contribuição à análise de sistemas de aterramento em meios horizontalmente estratificados.* Ph.D. thesis, Universidade Federal de Uberlândia. doi:10.14393/ufu.te.2019.2045. In portuguese.

Datsios, Z.G., Mikropoulos, P.N., Teneketzoglou, A., and Tzikas, D. (2014). Safety performance evaluation of fence grounding configurations in high voltage installations. In *2014 49th International Universities Power Engineering Conference (UPEC)*, 1–6. doi:10.1109/UPEC.2014.6934650.

Gazzana, D.S., Tronchoni, A.B., Leborgne, R.C., Telló, M., and Bretas, A.S. (2019). Numerical technique to the evaluation of multiple grounding electrodes coupled by the soil in high voltage substations. In *2019 IEEE International Conference on Environment and Electrical Engineering and 2019 IEEE Industrial and Commercial Power Systems Europe (EEEIC / I CPS Europe)*, 1–5. doi:10.1109/EEEIC.2019.8783554.

IEEE Std 80 (2015). Ieee guide for safety in ac substation grounding. *IEEE Std 80-2013 (Revision of IEEE Std 80-2000/ Incorporates IEEE Std 80-2013/Cor 1-2015)*, 1–226. doi:10.1109/IEEESTD.2015.7109078.

NBR 15751 (2013). *Sistemas de aterramento de subestações - Requisitos.* Associação Brasileira de Normas Técnicas (ABNT), ICS 17.220.20;29.080.10, Rio de Janeiro.

Pereira Fº, M.L. (1999). *Aplicação do método das imagens complexas ao cálculo de malhas de aterramento em solos com estratificação horizontal.* Master's thesis, Escola Politécnica, Universidade de São Paulo- USP. doi:10.11606/D.3.1999.tde-30112004-171403.